B3LYP Investigation of HPO_2, *trans*-HOPO, *cis*-HOPO, and Their Radical Anions

Nicole R. Brinkmann and Ian Carmichael*

Radiation Laboratory, University of Notre Dame, Notre Dame, Indiana 46556

Received: March 15, 2004

The B3LYP density functional method was used to determine the optimized geometries, harmonic vibrational frequencies, and anharmonic vibrational frequencies of HPO_2 and the trans- and cis-isomers of HOPO. Additionally, the isotropic hyperfine splitting (hfs) constants and the vibrationally averaged hfs were determined for the radical anions of each species. *cis*-HOPO is predicted to be the lowest energy isomer of the neutral systems, with *trans*-HOPO lying 3.0 kcal mol^{-1} higher and HPO_2 lying 11.9 kcal mol^{-1} higher than that. The pyramidal HPO_2^- radical is the lowest energy anion, and the cis- and trans-isomers lie ∼5 and ∼8 kcal mol^{-1}, respectively, above HPO_2^-. Higher lying σ radicals of $HOPO^-$ resemble PO_2^- and free H. The B3LYP/6-311+G(2d,2p) values of $A_{iso}(^1H)$ = 1211.98 MHz (trans) and 1199.90 MHz (cis) confirm that the $^2A'$ HOPO anion dissociates to PO_2^- + H. H_2PO was also investigated because of its similarity to HPO_2^-. The computed hfs constant for ^1H (109.64 MHz) is fortuitously in excellent agreement with the experimental value, while that for ^{31}P (950.29 MHz) differs significantly from experiment, and this deviation is attributed to the lack of a basis set for P that provides a good description of the P 1s core. Vibrational averaging affects the computed hfs in H_2PO by 5−6 MHz for $A_{iso}(^{31}P)$ but only by ∼2 MHz in HPO_2^-. The effect of vibrational averaging is small (1−2 MHz) for $A_{iso}(^1H)$ but more significant (8−20 MHz) in HPO_2^-. $A_{iso}(^{17}O)$ is relatively unaffected by vibrational averaging in both H_2PO and HPO_2^-. Solvent effects were evaluated using the conductor-like polarizable continuum model (CPCM), and these hfs values for HPO_2^- [$A_{iso}(^{31}P)$ = 1123.42 MHz, $A_{iso}(^1H)$ = 243.51 MHz] and H_2PO [$A_{iso}(^{31}P)$ = 1003.54 MHz, $A_{iso}(^1H)$ = 109.27 MHz] are in closer agreement with experiment. Convergence of the Fermi contact terms for ^{31}P computed using B3LYP with the aug-cc-pCVXZ and aug-cc-pV(X+d)Z families of basis sets is erratic and slow. On the other hand, with the same basis sets, CCSD(T) produces hfs constants for the P atom that are in close agreement with experiment.

I. Introduction

Dioxophosphoranes (three-coordinate phosphoryl derivatives, RPO_2) have long been considered as transient species or reaction intermediates. Some dioxophosphoranes are important intermediates in combustion chemistry,[1] while others have a key role in biological phosphorylation.[2] Dioxophosphoranes can even be strong enough phosphorylating agents to react with OH groups on the surface of some solids.[3] In 1991, Bodalski and Quin[4] reported that some dioxophosphoranes attack epoxides, first forming a Lewis salt and then rearranging to form five-membered cyclic phosphates. As a result of the strong electrophilic character of phosphorus in these systems, dioxophosphoranes can undergo self-reaction, polymerizing to form linear chains or cyclic systems (eq 1). Although the interest in low-coordination P-containing systems has grown and many have been successfully synthesized, dioxophosphoranes have remained elusive.[5]

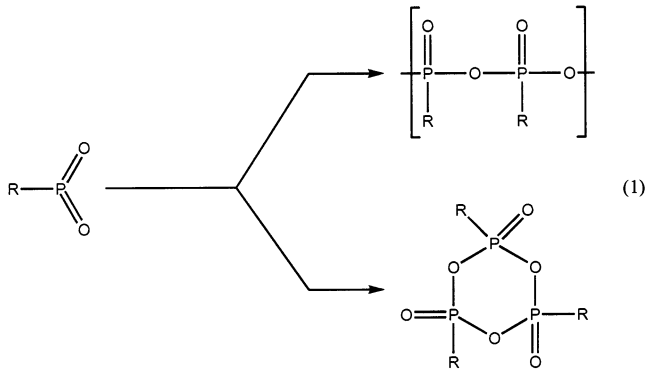

(1)

Despite such interest in phosphoranes and molecules containing group 15 atoms with low coordination numbers, very few possible RPX_2 isomers (where R = H or Cl and X = O, S, or Se) have been experimentally isolated. In particular, the tricoordinated planar phosphorane and the *cis*- and *trans*-phosphorine conformers (Figure 1) of HPO_2 have garnered both theoretical[6−9] and experimental[10−14] interest. In 1986, Schoeller and Lerch[7] reported SCF/DZP results showing that metaphosphorus acid (HPO_2) exhibits allylic-type bonding (consistent with having strong dipolar character) as opposed to having multiple bond character at the phosphorus center (Figure 1a,b). Miller and Stevens-Miller[15] derived the gas phase acidity of HPO_2 as 1376 ± 17 kJ mol^{-1} by studying the endothermic reaction $PO_2^- + HCl \rightarrow Cl^- + HPO_2$ in a flow-drift tube. The most recent experimental work on metaphosphorus acid was in 1994 when Hildenbrand and Lau[12] reacted $H_2O(g)$ with $Ca_2P_2O_7(s)$ and identified HPO_2 by mass spectroscopy. HPO_2 was then thermochemically characterized from several reaction equilibria, and the standard enthalpy of formation was reported as −110.6 ± 3 kcal mol^{-1}.[12] The radical anion HPO_2^- was first identified in 1962 by Morton;[16] there has been little experimental information about this molecular system available since then. Behar and Fessenden[17] produced HPO_2^- from radiolysis of an aqueous solution of $OH + H_2PO_2^-$, and their electron para-

10.1021/jp0402176 CCC: $27.50
Published on Web 10/01/2004

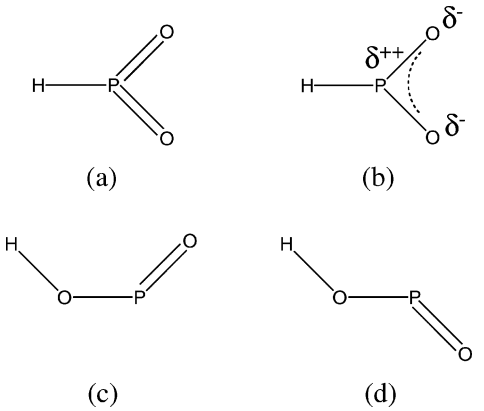

Figure 1. (a) C_{2v} isomer of HPO_2 with multiple bonding at the P center versus (b) allylic-type bonding in HPO_2; (c) cis- and (d) trans-isomers of HOPO.

magnetic resonance (EPR) results were similar to those obtained by the crystal experiments of Morton.

At the CI/TZP level of theory, Mathieu, Navech, and Barthelat[9] reported an energetic ordering of *cis*-HOPO < *trans*-HOPO < HPO_2, with the trans-isomer and HPO_2 lying 3.9 and 15.0 kcal mol^{-1}, respectively, higher than *cis*-HOPO. It is generally accepted that the cis-conformer is the most stable, and it has been studied experimentally more thoroughly than the other isomers. *cis*-HOPO is a final product in the combustion of organophosphorus compounds,[18] it is the main product in the destruction of trimethyl phosphate and dimethyl methyl phosphate,[19] and it is a catalyst for the reaction $OH + H_2 \rightarrow H_2O + H$.[13] *cis*-HOPO has also been identified as a primary depolymerization product of phosphorus oxides[11] and as a hydrolysis intermediate in the depolymerization of orthorhombic P_4O_{10}.[11] In 1988, Withnall and Andrews[10] measured the IR spectroscopy of the $O + PH_3$ reaction products (including *cis*-HOPO) trapped in solid Ar, and in 2000, Bell and co-workers[20] detected the transient HOPO in the gas phase using high-resolution IR laser absorption spectroscopy.

While information on HPO_2 and HOPO is rather limited, even less is known about the radical anions of these systems. Thus, we undertook a quantum chemical investigation of HPO_2 and HPO_2^- and *cis*- and *trans*-HOPO and $HOPO^-$. A brief comment is also made on the pyramidal radical H_2PO in comparison to the pyramidal HPO_2^-. Contrasts are also drawn with results from recent work on some nitrogen-based isoelectronic species.

II. Methods

All quantum chemical computations were performed on HPO_2, *cis*- and *trans*-HOPO, and their respective anions using the Gaussian 98[21] and Gaussian 03[22] program packages. The gradient-corrected functional, denoted B3LYP, was used to compute the geometries, energies, harmonic vibrational frequencies, anharmonic vibrational fundamentals, the hyperfine splitting constants at the equilibrium structures and at the vibrationally averaged structures, and the *g*-factors of the vibrationally averaged structures. Energies were converged to at least 10^{-6} hartrees in the self-consistent field procedures, although the absolute accuracy may be somewhat lower due to numerical integration procedures. The anharmonic vibrational fundamentals reported using Gaussian 03 are computed via a perturbational approach. B3LYP is a hybrid Hartree−Fock and density functional theory (HF/DFT) method that uses Becke's three-parameter exchange functional (B3)[23] with the Lee, Yang, and Parr correlation functional (LYP).[24] The coupled cluster with single and double excitations and with perturbatively applied triple excitations [CCSD(T)][25−27] theory was used to compute the hyperfine splitting constants of the P atom. An unrestricted Hartree−Fock reference was used for all correlated procedures. To compute the *g*-factor in solution, the conductor-like polarizable continuum model (CPCM)[28,29] was used.

A 6-31+G* basis set was used in the preliminary geometry optimizations. This basis set was formed from the 6-31 basis set of Hehre et al.[30] and Francl et al.[31] combined with the polarization and diffuse functions of Frisch et al.[32] and Clark et al.[33] These basis sets have contraction schemes of H(4s/2s), O(11s5p1d/4s3p1d), and P(16s10p1d/4s3p1d). The larger 6-311+G(2d,2p) basis set was subsequently used to compute the anharmonic fundamental vibrational frequencies of *cis*-HOPO for which experimental fundamental frequencies are known. This basis set is obtained for H and O from the 6-311 basis of Hehre et al.[34] by adding diffuse functions and two sets of d functions on oxygen atoms and two sets of p functions on hydrogen. The 6-311+G(2d,2p) basis set for P is based on the McLean−Chandler[35] basis set with diffuse functions and two sets of d functions on phosphorus. The EPR-II basis set of Barone[36] was used for H and O for computing the Fermi contact terms of the radicals. This basis set is a double-ζ basis set with a single set of polarization functions and an enhanced s part. The contraction schemes for this basis set are H(6s1p/4s1p) and O(10s5p1d/6s2p1d).

The correlation-consistent polarized core−valence family of basis sets of Woon and Dunning[37] augmented with diffuse functions following Kendall et al.[38] (aug-cc-pCVXZ) and the newer family of correlation-consistent basis sets of Dunning, Peterson, and Wilson[39] which include tight d functions and a systematic expansion of the higher angular moment functions [aug-cc-pV(X+d)Z] were used to systematically investigate the Fermi contact terms of the HPO_2^- and H_2PO radicals and the P atom. For HPO_2^-, The aug-cc-pCVXZ basis sets range in size from 99 contracted Gaussian basis functions (aug-cc-pCVDZ) to 398 (aug-cc-pCVQZ). For HPO_2, this range is 88−335. The valence "plus d" sets range from 87 [aug-cc-pV(D+d)Z] to 470 functions [aug-cc-pV(Z+d)Z] for HPO_2^- and from 73 to 423, respectively, for HPO_2.

Geometries were optimized for each molecular system with the B3LYP functional using analytic gradient techniques. Residual Cartesian gradients were $<1.5 \times 10^{-5}$ hartrees/b. Stationary points found in optimizations were confirmed as minima by computing the harmonic vibrational frequencies using analytic second derivatives.

III. Results and Discussion

A. Structures and Relative Energies. The B3LYP optimized structures of the neutral and anionic tricoordinated phosphorane HPO_2 are given in Figure 2a. The neutral species is a planar $^1A_1$ C_{2v} structure. The planar $^2B_1$ anion is a transition state with one imaginary frequency leading to the pyramidal $^2A'$ state in C_s symmetry which is the minimum on the potential energy surface of the anion. The harmonic vibrational frequencies and the theoretical anharmonic fundamental vibrational frequencies of HPO_2 and both the planar and pyramidal anions are given in Table 1. The P−H and P−O bond distances are ~0.06 Å longer in the anion (1.460 Å; 1.519 Å) than in the neutral species (1.401 Å; 1.460 Å). With the 6-311+G(2d,2p) basis set, the O atoms are bent 56.4° out of the plane of the C_{2v} structure.

The B3LYP optimized structures of *cis*- and *trans*-HOPO and the corresponding radical anions are shown in Figure 2b. These systems are all planar. The lowest unoccupied molecular orbital

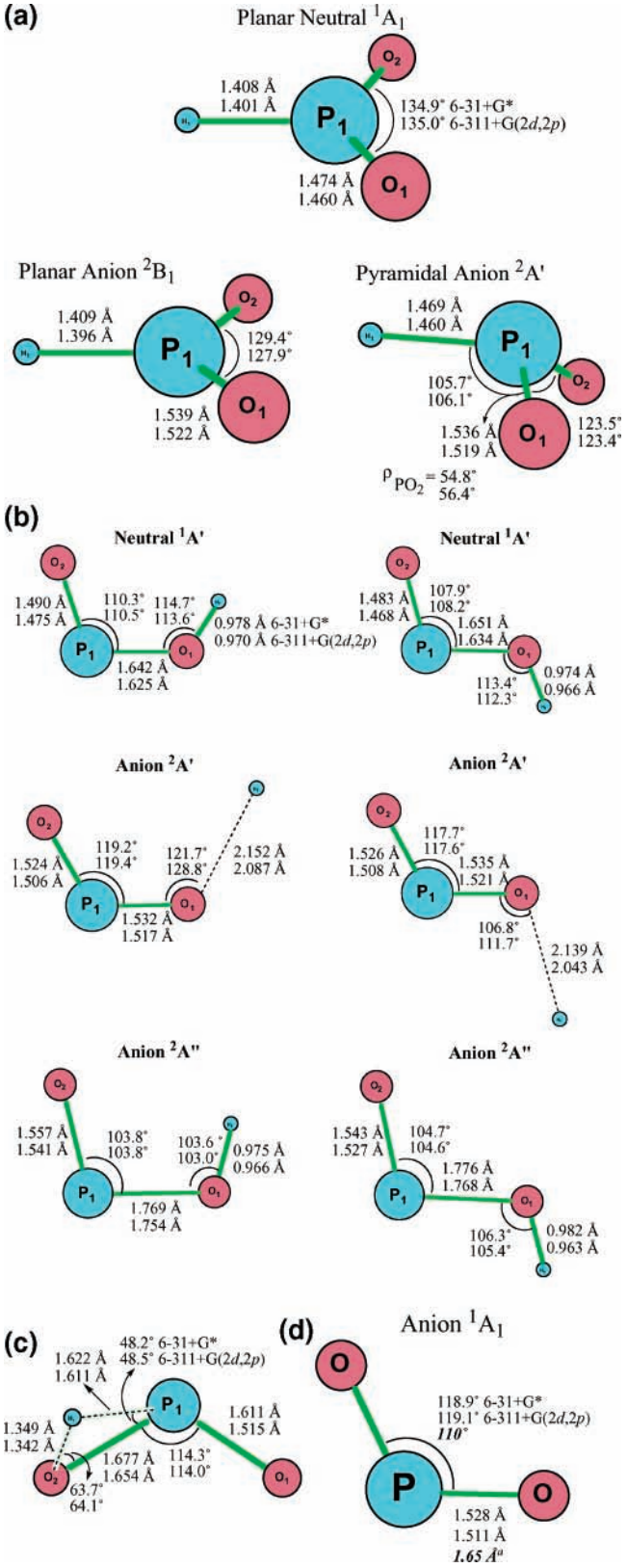

Figure 2. B3LYP/6-31+G* optimized structures of (a) HPO_2 and HPO_2^-, (b) the cis- and trans-isomers of HOPO and $HOPO^-$, (c) the transition state between HPO_2^- and *cis*-$HOPO^-$, and (d) PO_2^-.

of HOPO is A″, and the next lowest is A′. Correspondingly, for both isomers of $HOPO^-$, a π radical ($^2A''$) and a higher lying σ radical ($^2A'$) are found. A transition state for the hydrogen shift between HPO_2^- and *cis*-$HOPO^-$ was located and is shown in Figure 2c. The π radicals show a slightly long central O−P bond (1.754 Å, cis; 1.768 Å, trans). This is similar

TABLE 1: Harmonic Vibrational Frequencies (cm^{-1}) and Anharmonic Fundamental Vibrational Frequencies (cm^{-1}) for HPO_2 and HPO_2^- [a]

		HPO_2 ($^1A_1$)	HPO_2^- ($^2B_1$)	HPO_2^- ($^2A'$)
		A_1	A_1	A'
ω_1	6-31+G*	2504	2458	1987
ν_1		2384	2246	1853
ω_1	6-311+G(2d,dp)	2461	2476	1950
ν_1		2351	2249	1813
ω_2	6-31+G*	1124	936	1150
ν_2		1110	926	1130
ω_2	6-311+G(2d,dp)	1136	958	1169
ν_2		1123	945	1149
ω_3	6-31+G*	453	389	976
ν_3		449	382	961
ω_3	6-311+G(2d,dp)	456	402	991
ν_3		453	394	977
		B_1	B_1	
ω_4	6-31+G*	603	[1526]	761
ν_4		608	[1804]	740
ω_4	6-311+G(2d,dp)	612	[1579]	760
ν_4		615	[1899]	739
		B_2	B_2	
ω_5	6-31+G*	1436	1181	410
ν_5		1415	1164	407
ω_5	6-311+G(2d,dp)	1448	1192	418
ν_5		1428	1176	415
				A''
ω_6	6-31+G*	1013	943	918
ν_6		1003	917	888
ω_6	6-311+G(2d,dp)	986	937	904
ν_6		978	905	872

[a] Imaginary frequencies are in brackets.

to the findings of van Doren et al.[40] for the radical anions from *cis*- and *trans*-nitrous acid, where elongated central O−N bonds foreshadow dissociation into OH^- and NO. The association energy of OH^- + PO is 25.92 kcal mol^{-1} (cis) and 22.39 kcal mol^{-1} (trans). A counterpoise correction changes these by 3.07 and 3.03 kcal mol^{-1}, respectively. In contrast, the σ radicals of both isomers show an elongated O−H bond (2.087 Å, cis; 2.043 Å, trans), indicating dissociation of free H, leaving the PO_2^- anion. The association energy of H + PO_2^- is 1.65 kcal mol^{-1}, and a counterpoise correction makes a difference of 0.60 kcal mol^{-1}. The B3LYP optimized structure of PO_2^- is given in Figure 2d for comparison.

The harmonic vibrational frequencies and computed anharmonic fundamental vibrational frequencies of HOPO and $HOPO^-$ are given in Table 2; the computed harmonic frequencies and anharmonic fundamental vibrational frequencies for PO_2^- are included for comparison. Available experimental fundamental frequencies for *cis*-HOPO and PO_2^- are also given. With the 6-311+G(2d,2p) basis set, there is close agreement between the theoretical anharmonic frequencies and the experimental fundamentals. The comparison of ν_1 (1156 cm^{-1}, trans; 1165 cm^{-1}, cis; 1170 cm^{-1}, PO_2^-), ν_2 (1021 cm^{-1}, trans; 1023 cm^{-1}, cis; 1030 cm^{-1}, PO_2^-), and ν_3 (420 cm^{-1}, trans; 442 cm^{-1}, cis; 446 cm^{-1}, PO_2^-) confirms the dissociation of H from PO_2^- in the σ radicals of the *trans*- and *cis*-$HOPO^-$ isomers. The frequencies of the π radicals are consistent with the notion that the unpaired electron in the $^2A''$ anions is in an orbital perpendicular to the plane of the molecule. Interestingly, the A″ mode of $^2A''$ *trans*-$HOPO^-$ is imaginary when computed with the 6-31+G* basis set. When computed with the larger 6-311+G(2d,2p) basis set, the harmonic vibrational frequency is predicted to be imaginary as well; however, the computed

TABLE 2: Harmonic Vibrational Frequencies (cm^{-1}) and Anharmonic Fundamental Vibrational Frequencies (cm^{-1}) for *trans*-HOPO, *cis*-HOPO, the Corresponding Anions, and PO_2^- [a]

		HOPO ($^1A'$)		*trans*-HOPO$^-$		*cis*-HOPO$^-$		PO_2^-
		trans	cis	($^2A'$)	($^2A''$)	($^2A'$)	($^2A''$)	($^1A_1$)
		A′	A′	A′	A′	A′	A′	B_2
ω_1	6-31+G*	3718	3663	1157	3718	1168	3692	1172
ν_1		3529	2472	1144	3515	1151	3499	1155
ω_1	6-311+G(2d,2p)	3796	3742	1170	3809	1181	3775	1187
ν_1		3608	3549	1156	3613	1165	3595	1170
			3551[b]					1207[c]
								A_1
ω_2	6-31+G*	1265	1242	1023	1066	1026	1042	1031
ν_2		1251	1227	1012	1045	1013	1023	1018
ω_2	6-311+G(2d,2p)	1279	1241	1031	1078	1034	1057	1043
ν_2		1265	1241	1021	1055	1023	1042	1030
			1253[b]					1097[c]
								A_1
ω_3	6-31+G*	925	942	466	939	448	950	445
ν_3		851	900	423	850	436	930	442
ω_3	6-311+G(2d,2p)	964	919	489	962	452	969	449
ν_3		937	*919*	420	848	442	963	446
								501[c]
ω_4	6-31+G*	799	818	345	580	374	607	
ν_4		785	803	271	565	272	592	
ω_4	6-311+G(2d,2p)	804	820	374	570	408	594	
ν_4		788	804	310	552	366	578	
			842[b]					
ω_5	6-31+G*	396	377	158	333	141	325	
ν_5		395	374	101	329	120	305	
ω_5	6-311+G(2d,2p)	407	389	168	342	121	333	
ν_5		404	386	105	332	143	307	
		A″	A″	A″	A″	A″	A″	
ω_6	6-31+G*	485	565	77	[78]	[33]	243	
ν_6		485	565	12	[157]	[252]	177	
ω_6	6-311+G(2d,2p)	481	561	83	[95]	50	222	
ν_6		450	541	164	465	189	417	
			524[b]					

[a] Imaginary frequencies are in brackets. Available experimental fundamental frequencies are included. [b] Reference 20. [c] References 10 and 62.

fundamental vibrational frequency is real and similar in magnitude to that computed for *cis*-HOPO$^-$.

The total electronic energies of the neutral molecules and the anions at the B3LYP/6-31+G* and B3LYP/6-311+G(2d,2p) levels are given in Table 3. Relative energies are listed in kcal mol^{-1}. In the neutral systems, *cis*-HOPO is the most stable conformation, with the trans-isomer lying 3.0 kcal mol^{-1} higher and HPO_2 lying 11.9 kcal mol^{-1} above that. The pyramidal, tricoordinated HPO_2^- is the most stable anion, with $^2A''$ *cis*-HOPO$^-$ ~5 kcal mol^{-1} higher and $^2A''$ *trans*-HOPO$^-$ another 3 kcal mol^{-1} higher. PO_2^- + H ($^2A'$ *cis*- and *trans*-HOPO$^-$) lies ~33 kcal mol^{-1} above HPO_2^-. The adiabatic electron affinity (AEA) was determined as the difference in the total electronic energy of the optimized neutral system minus that of the optimized anion. The π radical anions of *cis*- and *trans*-HOPO are bound [AEA(cis) = 0.46 eV and AEA(trans) = 0.46 eV]. The AEA of HPO_2 is 1.33 eV. With zero-point correction, these values are 0.51 eV (cis), 0.52 eV (trans), and 1.38 eV (HPO_2). The vertical electron affinity (VEA) was determined as the difference in the total electronic energy of the optimized neutral system minus that of the anion at the geometry of the optimized neutral system, and this value for *cis*- and *trans*-HOPO is 0.16 and 0.20 eV, respectively. The VEA of HPO_2 is 0.30 eV.

B. Hyperfine Splitting Constants. From his EPR investigation,[16] Morton reported that the HPO_2^- radical is pyramidal, with the unpaired electron localized on the phosphorus atom in a hybrid σ orbital. The computed isotropic hyperfine splitting (hfs) constants for the planar $^2B_1$ and pyramidal $^2A'$ HPO_2^- are given in Tables 4 and 5, respectively. The 6-31+G* and 6-311+G(2d,2p) values of $A_{iso}(^1H)$ = 230.53 and 229.07 MHz for $^2A'$ HPO_2^- are in close agreement with Morton's average experimental value of 230 MHz, but this agreement may be fortuitous, since the EPR-II/6-311+G(2d,2p) value of 257 MHz deviates from experiment by almost 30 MHz. In solution, the Fermi contact term for ^1H is 270.98 MHz (6-31+G*), 247.91 MHz [6-311+G(2d,2p)], and 243.51 MHz [EPR-II/6-311+G(2d,2p)], all of which are in close accord with the experimental solution phase value of 252 MHz.[17] However, the computed hfs constant for ^{31}P (880.29 MHz) compares poorly with the experimental value of 1385 MHz. The larger basis sets improve the computed value to 1063.76 MHz [6-311+G(2d,2p)] and 1065.32 MHz [EPR-II/6-311+G(2d,2p)], but these values are still ~300 MHz different from experiment. In solution, the computed values of $A_{iso}(^{31}P)$ all move toward experiment [1108.73 MHz, 6-31+G*; 953.60 MHz, 6-311+G(2d,2p); 1123.42 MHz, EPR-II/6-311+G(2d,2p)]. The remaining deviation is most likely a consequence of the deficiencies in the available basis sets for adequately describing the 1s core of the phosphorus atom.

Deficiencies in structural predictions were observed by Wesolowski et al.[41] in a high-level theoretical investigation of H_3PO and H_2POH. It was noted that the conventional Dunning correlation-consistent polarized valence (cc-pVXZ)[42−45] basis sets fail to provide correct results for these P-containing systems even when used with a high level of theory such as coupled-cluster singles and doubles with perturbatively applied triple excitations. Results were improved with the inclusion of tight d functions by using Dunning's core−valence (cc-pCVXZ)[37] or the plus d [cc-pV(X+d)Z][39] basis sets. In subsequent work, Tackett and Clouthier[46] reported difficulties in obtaining reliable excitation energies for HPO with all but very large basis sets and high levels of theoretical methods. With this in mind, the aug-cc-pCVXZ and aug-cc-pV(X+d) basis sets were used to compute the Fermi contact terms of HPO_2^- using the optimized geometry obtained at the B3LYP/6-311+G(2d,2p) level. These values are also given in Table 5. Graphs of these data are shown in Figures 3 and 4.

The trends in the values of $A_{iso}(^{17}O)$ computed with the two families of basis sets are given in Figures 3a and 4a, and with the aug-cc-pCVXZ basis sets, it appears that this value is converging to about −20 MHz. With the aug-cc-pV(X+d)Z basis sets, the aug-cc-pV(D+d)Z through aug-cc-pV(Q+d)Z values also appear to be converging to about −12 MHz, although from the opposite direction as that with the aug-cc-pCVXZ basis sets. However, the (5+d)Z value drops back down to −16.54 MHz, and it is suspected that if the aug-cc-pCV5Z basis set were available, this value would drop to −18 or −19 MHz, leaving convergence still somewhat nebulous. Figures 3b and 4b show even more troubling trends for $A_{iso}(^{31}P)$ computed with these basis sets. With the aug-cc-pCVXZ basis set, there is a large jump between the aug-cc-pCVTZ value (987.46 MHz) and the aug-cc-pCVQZ value (1011.42 MHz). The aug-cc-pV(X+d)Z values do not show a convergence trend. However, the values do appear to be "sandwiched" between the aug-cc-pV(D+d)Z value of 922.89 MHz and the aug-cc-pV(5+d)Z value of 968.52 MHz. Graphs of $A_{iso}(^1H)$ computed with both

TABLE 3: B3LYP Total Electronic Energies (E_h Values) for HPO_2, *trans*-HOPO, *cis*-HOPO, and the Corresponding Anions[a]

		neutral	anion	
		HPO_2		
AEA = 1.43 eV	6-31+G*	−492.412 187	−492.464 620	
(1.04 eV)		[16.0]	[0.0]	
1.33 eV	6-311+G(2d,2p)	−492.504 705	−492.553 454	
(1.38 eV)		[14.9]	[0.0]	
VEA = 0.13 eV	6-31+G*			
0.30 eV	6-311+G(2d,2p)			
		trans-HOPO		
			$^2A'$	$^2A''$
AEA = 0.57 eV	6-31+G*	−492.431 926	−492.412 430	−492. 452 946
(0.63 eV)		[3.6]	[32.8]	[7.3]
0.46 eV	6-311+G(2d,2p)	−492.523 586	−492.500 985	−492.540 636
(0.52 eV)		[3.0]	[32.9]	[8.04]
VEA = 0.31 eV	6-31+G*			
0.20 eV	6-311+G(2d,2p)			
		cis-HOPO		
			$^2A'$	$^2A''$
AEA = 0.58 eV	6-31+G*	−492.437 633	−492.412 562	−492. 458 764
(0.62 eV)		[0.0]	[32.7]	[3.7]
0.46 eV	6-311+G(2d,2p)	−492.528 402	−492.501 448	−492.545 333
(0.51 eV)		[0.0]	[32.6]	[5.1]
VEA = 0.27 eV	6-31+G*			
0.16 eV	6-311+G(2d,2p)			

[a] Relative energies (kcal mol^{-1}) are listed in brackets. Adiabatic and vertical electron affinities (AEAs and VEAs, respectively) are given in eV. Zero-point corrected values are in parentheses. The EAs for the trans- and cis-isomers are to the lower energy $^2A''$ state.

TABLE 4: Isotropic Fermi Contact Couplings (MHz) for the $^2B_1$ State of HPO_2^- Using B3LYP[a]

$^2B_1$ HPO_2^-		$^{17}O_1$	$^{17}O_2$	^{31}P	^1H
6-31+G*		−27.21	−27.21	163.93	−27.21
	0 K	*−29.66*	*−29.66*	*260.62*	*−63.03*
	298 K	*−29.71*	*−29.71*	*261.81*	*−51.13*
6-311+G(2d,2p)		−19.95	−19.95	205.75	−68.03
	0 K	*−22.71*	*−22.71*	*235.98*	*−53.17*
	298 K	*−22.78*	*−22.78*	*236.98*	*52.84*
EPR-II [H,O],		−25.95	−25.95	214.64	−73.52
6-311+G(2d,2p) [P]	0 K	*−29.63*	*−29.63*	*291.25*	*−54.97*
	298 K	*−29.71*	*−29.71*	*292.87*	*−54.97*

[a] Vibrationally averaged values were computed at 0 and 298 K and are in italics.

TABLE 5: Isotropic Fermi Contact Couplings (MHz) for the $^2A'$ State of HPO_2^- Using B3LYP[a]

$^2A'$ HPO_2^-		^{17}O	^{31}P	^1H
6-31+G*		−29.39	880.29	230.53
	0 K	*−29.48*	*880.30*	*250.92*
	298 K	*−29.29*	*878.52*	*237.67*
	CPCM	−31.66	953.60	247.91
6-311+G(2d,2p)		−23.54	1063.76	229.07
	0 K	*−23.47*	*1061.29*	*235.98*
	298 K	*−23.47*	*1061.23*	*236.14*
	CPCM	−26.34	1123.42	243.51
EPR-II [H,O],		−28.11	1065.32	257.44
6-311+G(2d,2p) [P]	0 K	*−28.04*	*1063.40*	*265.28*
	298 K	*−28.04*	*1063.35*	*265.46*
	CPCM	−30.44	1108.73	270.98
aug-cc-pV(D+d)Z		−30.28	922.89	233.07
aug-cc-pV(T+d)Z		−12.72	964.74	252.60
aug-cc-pV(Q+d)Z		−12.29	933.67	261.32
aug-cc-pV(5+d)Z		−16.54	968.52	271.21
aug-cc-pCVDZ		−13.04	985.91	231.31
aug-cc-pCVTZ		−19.48	987.46	252.77
aug-cc-pCVQZ		−19.96	1011.42	261.14
aug-cc-pCVDZ+1s		−13.05	964.28	231.22
aug-cc-pCVTZ+1s		−19.48	1003.83	252.77
aug-cc-PCVQZ+1s		−19.96	1003.80	261.14
TZVP		−25.95	1027.41	235.01
expt			1385[b]	230[b]
			1346[c]	252[c]

[a] Vibrationally averaged values were computed at 0 and 298 K and are in italics. Solution phase values were estimated using CPCM. Available experimental values are given. [b] Reference 16. [c] Reference 17.

families of basis sets [Figure 3c, aug-cc-pCVXZ; Figure 4c, aug-cc-pV(X+d)Z] show that these values are not converging.

While there are observed problems with the convergence of the Fermi contact terms for each nuclear center in HPO_2^-, these are most likely all consequences of the basis sets available for P. The B3LYP and CCSD(T) computed hfs constants for the ^4S P atom are given in Table 6, and graphs of the values with the aug-cc-pCVXZ and aug-cc-pV(X+d)Z basis sets are respectively shown in parts a and b of Figures 5 (B3LYP) and 6 [CCSD(T)]. The graphs of the B3LYP data show that the values of $A_{iso}(^{31}P)$ do not appear to converge smoothly, although the magnitude of the aug-cc-pCVQZ value of −51.13 MHz [which is similar to the 6-311+G(2d,2p) value of −51.79 MHz] is in reasonable agreement (in magnitude) with the experimental value of 55.1 MHz.[47] The aug-cc-pV(6+d)Z value is −68.79 MHz, which is ∼14 MHz greater than experiment.

In a study of the theoretical spin densities and hyperfine coupling in the atoms B−F,[48] it was reported that the B3LYP functional used with the aug-cc-pCVXZ basis sets produces limiting values for the N atom that are fortuitously close to experiment. While similar results might be expected for the isoelectronic P atom, the magnitude of the computed $A_{iso}(^{31}P)$ value is close to experiment, but the sign is opposite. The CCSD(T) data, however, converge to values of 52.00 MHz (aug-cc-pCVQZ) and 57.06 MHz [aug-cc-pV(5+d)], which are in good agreement with both the magnitude and sign of the experimental value.

Further attempts to increase the basis set flexibility in the core region by including energy optimized, high-exponent s functions with the aug-cc-pCVXZ basis sets led to little change in the predicted coupling constants computed for the P atom. However, when these modified basis sets were used for HPO_2^-, $A_{iso}(^{31}P)$ shows a nice convergence trend: 964.28 MHz (aug-

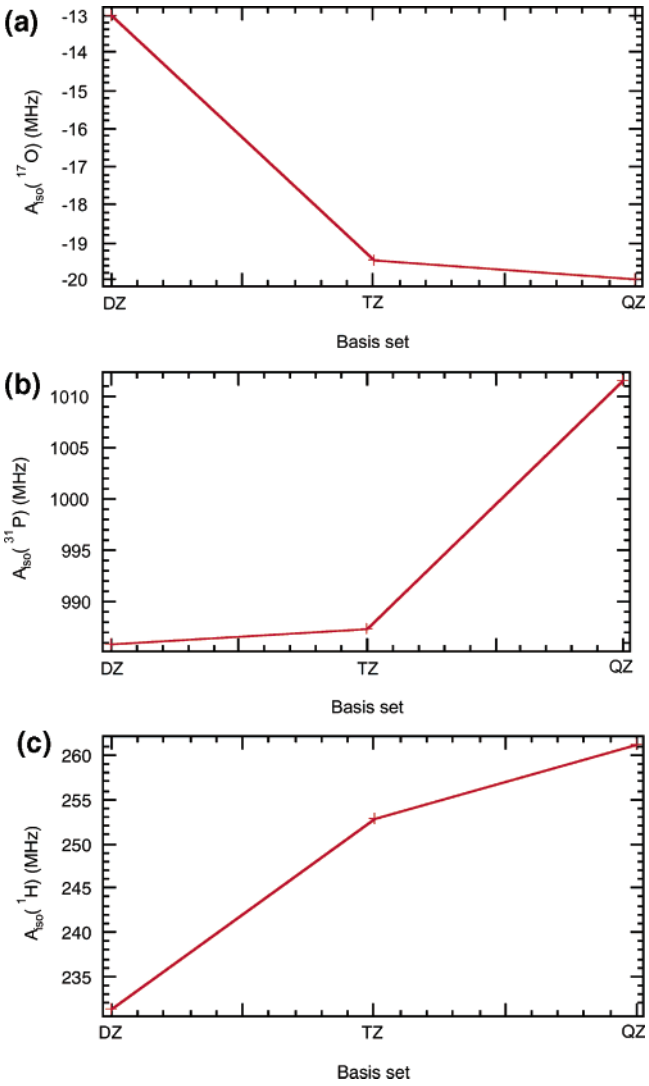

Figure 3. Isotropic hyperfine splitting constants of (a) ^{17}O, (b) ^{31}P, and (c) ^{1}H with the aug-cc-pCVXZ family of basis sets.

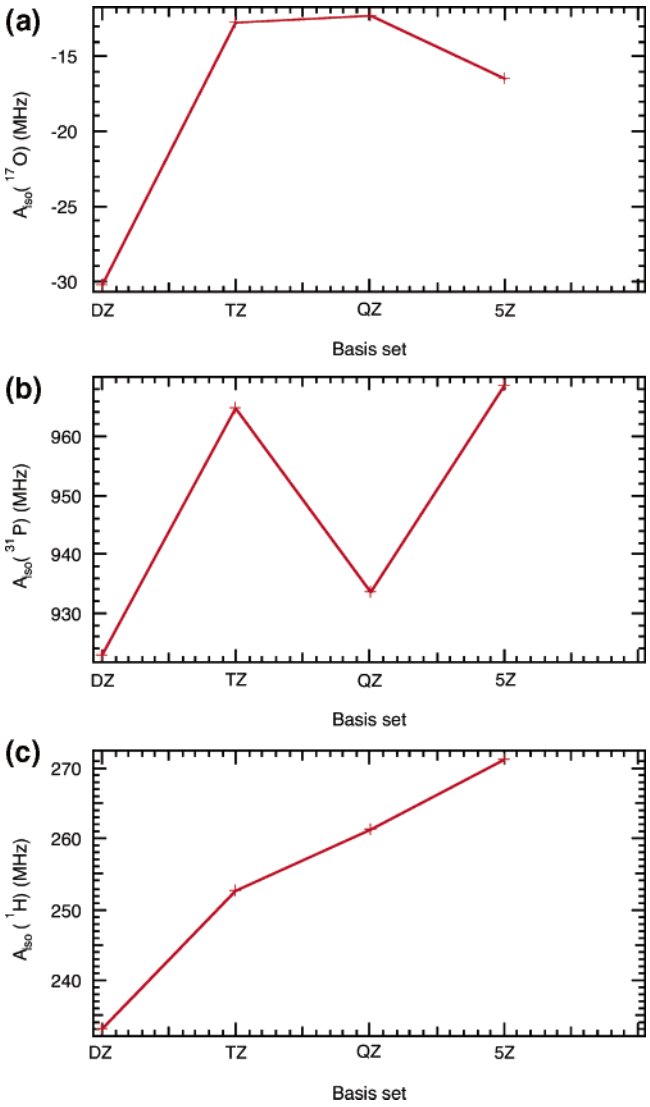

Figure 4. Isotropic hyperfine splitting constants of (a) ^{17}O, (b) ^{31}P, and (c) ^{1}H with the aug-cc-pV(X+d)Z family of basis sets.

cc-pCVDZ+1s), 1003.83 MHz (aug-cc-pCVTZ+1s), and 1003.80 MHz (aug-cc-pCVQZ+1s). While this value is still 350−400 MHz different from experiment, the convergence of this value is good.

In a study of P-containing radicals, Nguyen et al.[49] reported that the TZVP basis set of Godbout and co-workers[50] used with the B3LYP functional produces computed hfs constants that are in better agreement with experiment than the other basis sets included in their study. Thus, the Fermi contact terms for HPO_2^- were computed here at the B3LYP/TZVP level of theory, and these values are included in Table 5. The value of $A_{iso}(^{31}P) = 1027.41$ MHz is found to be in worse agreement with experiment than that computed with the 6-311+G(2d,2p) or EPR-II/6-311+G(2d,2p) basis sets, while $A_{iso}(^{1}H) = 235.01$ MHz is comparable to the 6-311+G(2d,2p) value and to experiment.

C. Vibrational Averaging and Solution Effects. It should also be noted that the static Fermi contact terms for ^{1}H vary from −27.21, −68.03, and −73.52 MHz [6-31+G*, 6-311+G(2d,2p), EPR-II/6-311+G(2d,2p), respectively] in the planar structure to 230.53, 229.07, and 257.44 MHz [6-31+G*, 6-311+G(2d,2p), EPR-II/6-311+G(2d,2p), respectively] in the pyramidal minimum. It is known that EPR parameters are strongly influenced by inversion motion at the radical center. Barone and co-workers[51−54] developed a numerical procedure to treat large-amplitude nuclear motions in nonrigid radicals. This method was applied to HPO_2^- in the present work. The primary effect of pyramidalization is an increase in the s character of the singly occupied molecular orbital (SOMO) at the radical center which is reflected by an increase in the hfs constants at ^{31}P and ^{1}H. These effects computed with the 6-31+G* basis set are shown in Figure 7. The barrier to inversion in HPO_2^- is ∼24 kcal mol^{-1} (Figure 8a), and thus, the vibrational averaging effects are less pronounced, since high barriers imply widely spaced vibrational states and smaller

TABLE 6: Isotropic Fermi Contact Couplings (MHz) for ^4S P Using B3LYP

	B3LYP	CCSD(T)
6-31+G*	−12.61	
6-311+G(2d,2p)	−51.79	
aug-cc-pV(D+d)Z	86.71	152.28
aug-cc-pV(T+d)Z	47.86	125.42
aug-cc-pV(Q+d)Z	1.51	74.86
aug-cc-pV(5+d)Z	−73.36	57.06
aug-cc-pV(6+d)Z	−68.79	
aug-cc-pCVDZ	48.81	156.73
aug-cc-pCVTZ	−65.99	23.67
aug-cc-pCVQZ	−51.13	52.00
expt	55.1[a]	

[a] Reference 47.

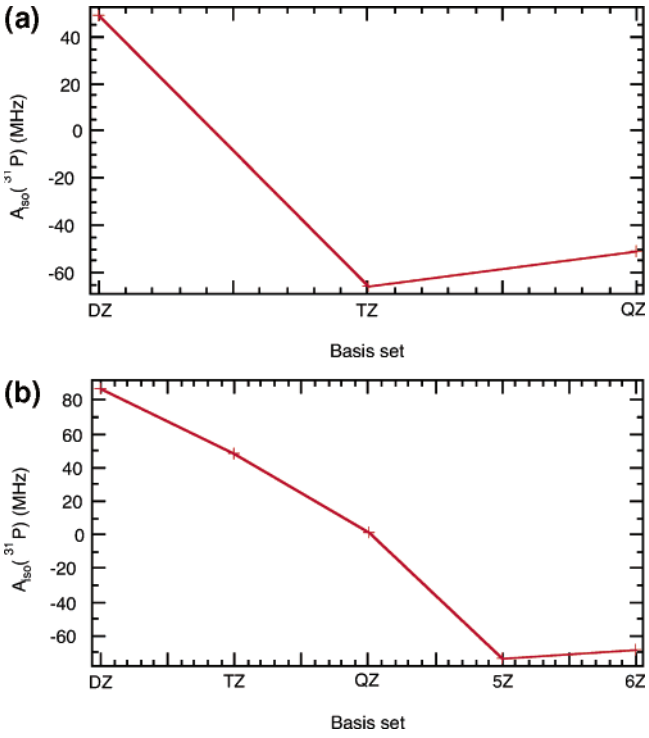

Figure 5. B3LYP isotropic hyperfine splitting constants of the ^4S ^{31}P atom with the (a) aug-cc-pCVXZ and (b) aug-cc-pV(X+d)Z families of basis sets.

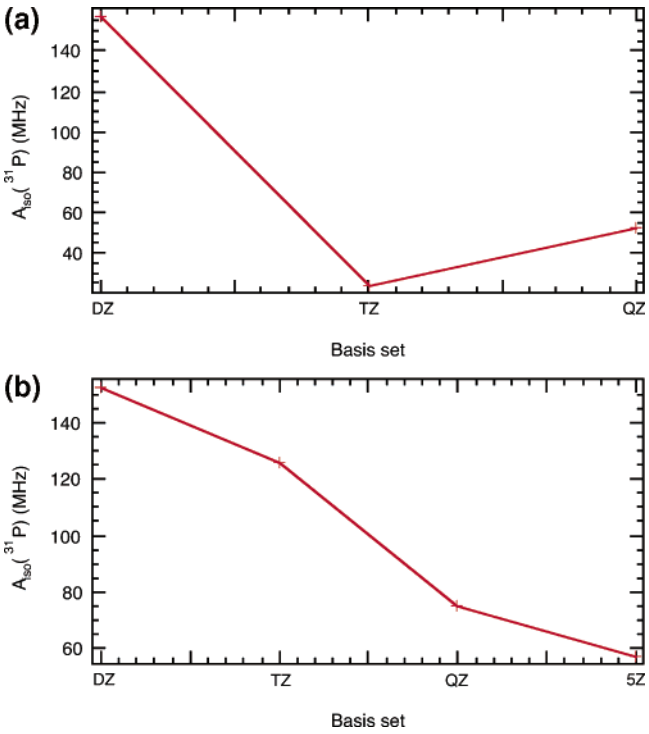

Figure 6. CCSD(T) isotropic hyperfine splitting constants of the ^4S ^{31}P atom with the (a) aug-cc-pCVXZ and (b) aug-cc-pV(X+d)Z families of basis sets.

average displacements from the equilibrium structure. In such a case, there is better agreement between the experimental Fermi contact terms and the static computed values. By way of contrast, in HNO_2^-, a low inversion barrier leads to large-amplitude motion and consequently large vibrational effects on the computed coupling constants.[55]

In HPO_2^-, the inclusion of vibrational averaging at 0 K causes little change observed for $A_{iso}(^{17}O)$ [−29.39 to −29.48 MHz

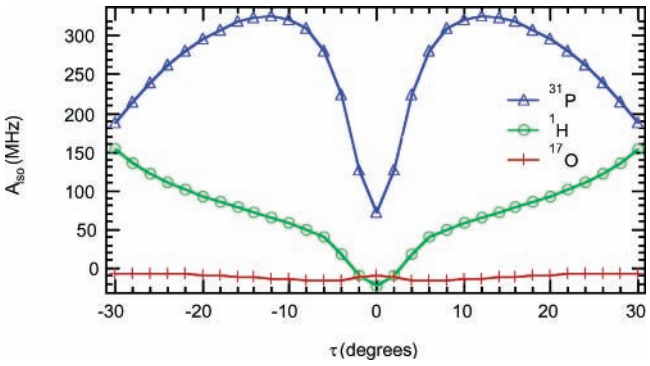

Figure 7. Isotropic hyperfine splitting constants of ^{31}P, ^1H, and ^{17}O of HPO_2 as a function of the degree of pyramidalization (τ).

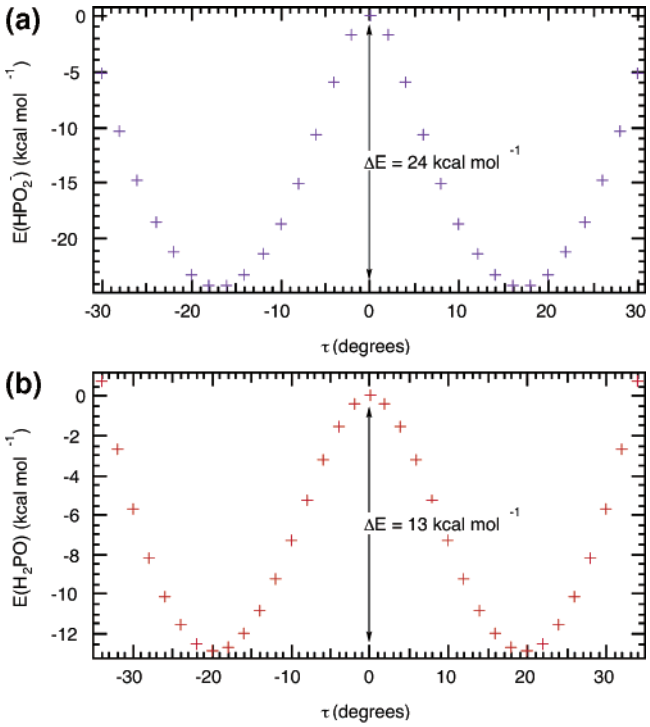

Figure 8. (a) Relative energy (kcal mol^{-1}) of HPO_2 as a function of the degree of pyramidalization (τ); (b) relative energy (kcal mol^{-1}) of H_2PO as a function of the degree of pyramidalization (τ).

with 6-31+G*; −23.54 to −23.47 MHz with 6-311+G(2d,2p); −28.11 to −28.04 MHz with EPR-II/6-311+G(2d,2p)] and $A_{iso}(^{31}P)$ [880.29 to 880.30 MHz with 6-31+G*; 1063.76 to 1061.29 MHz with 6-311+G(2d,2p); 1065.32 to 1063.40 MHz with EPR-II/6-311+G(2d,2p)]. However, vibrational averaging has a more significant effect on the Fermi contact term for ^1H [230.53 to 250.92 MHz with 6-31+G*; 229.07 to 235.98 MHz with 6-311+G(2d,2p); 257.44 to 265.46 MHz with EPR-II/6-311+G(2d,2p)]. Increasing the size of the basis set also has the most significant effect on $A_{iso}(^{31}P)$, which increases from ∼880 MHz with the 6-31+G* basis set to 1065.32 MHz with EPR-II/6-311+G*(2d,2p). Temperature affects are negligible for HPO_2^-. At 298 K, the hfs constants computed with the EPR-II/6-311+G(2d,2p) basis set are $A_{iso}(^{17}O) = -28.04$ MHz, $A_{iso}(^{31}P) = 1063.35$ MHz, and $A_{iso}(^1H) = 265.46$ MHz.

By comparison, vibrational averaging is important for accurately producing theoretical hfs constants for H in the nonrigid H_2PO radical. The Fermi contact terms of the dihydrophosphoryl radical (H_2PO) have been the subject[56−60] of considerable debate and interest for at least a decade. Most recently, Wesolowski et

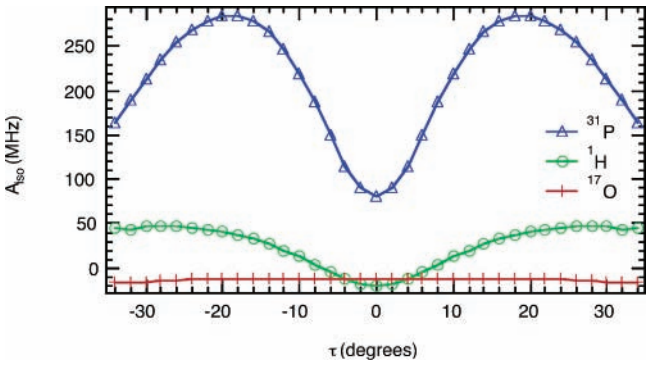

Figure 9. Isotropic hyperfine splitting constants of ^{31}P, ^{1}H, and ^{17}O of H_2PO as a function of the degree of pyramidalization (τ).

TABLE 7: Isotropic Fermi Contact Couplings (MHz) for the $^2A'$ State of H_2PO Using B3LYP[a]

$^2A'$ H_2PO		^{17}O	^{31}P	^{1}H
6-31+G*		−34.27	797.69	112.27
	0 K	*−34.34*	*792.95*	*113.95*
	298 K	*−34.34*	*792.77*	*114.01*
	CPCM	−33.07	852.39	112.83
6-311+G(2d,2p)		−19.71	956.41	107.86
	0 K	*−19.74*	*950.29*	*109.64*
	298 K	*−19.74*	*950.06*	*109.70*
	CPCM	−21.28	1003.54	108.73
EPR-II [H,O],		−23.13	951.90	120.50
6-311+G(2d,2p) [P]	0 K	*−23.18*	*946.12*	*122.46*
	298 K	*−23.18*	*945.92*	*122.53*
	CPCM	−24.74	993.37	121.42
aug-cc-pV(D+d)Z		−46.66	890.22	96.37
aug-cc-pV(T+d)Z		−10.41	923.68	107.37
aug-cc-pV(Q+d)Z		−9.05	893.96	111.63
aug-cc-pV(5+d)Z		−17.23	922.95	115.80
aug-cc-pCVDZ		−11.52	947.69	95.23
aug-cc-pCVTZ		−23.58	935.80	107.61
aug-cc-pCVQZ		−24.24	963.33	111.51
expt			1023.43[b]	109.27[b]

[a] Vibrationally averaged values were computed at 0 and 298 K and are in italics. Solution phase values were estimated using CPCM. Available experimental values are given. [b] Reference 61.

al.[60] used high levels of ab initio theory [CCSD(T)/TZ2P(f,d)] to investigate this radical. While reporting that "the predicted structure and properties of H_2PO greatly depend on the level of theory employed",[60] the authors neglected to consider the effects of vibrational averaging on the computed hfs constants. Their values of $A_{iso}(^{31}P) = 969.4$ MHz and $A_{iso}(^{1}H) = 90.7$ MHz deviated from experiment[61] (1023.43 and 109.27 MHz, respectively) by as much as 54 MHz. While the deviation for ^{31}P is once again likely due to a poor description of the 1s core in the phosphorus basis set, the discrepancy of almost 20 MHz for ^{1}H may, in part, be a result of neglecting the out-of-plane deviations at the radical center, which can directly affect the spin density and the hfs constant.

The barrier to inversion in H_2PO is only 12.9 kcal mol^{-1} (Figure 8b), and the hfs constants for ^{31}P and ^{1}H both increase with pyramidalization of this radical (Figure 9). The computed isotropic hfs constants for H_2PO are given in Table 7. Vibrational averaging has little effect on the Fermi contact term for ^{17}O [−34.27 to −34.34 MHz, 6-31+G*; −19.71 to −19.74 MHz, 6-311+G(2d,2p); −23.13 to −23.18 MHz, EPR-II/6-311+G(2d,2p)]. The effect on $A_{iso}(^{31}P)$ is ∼5 MHz [797.69 to 792.95 MHz, 6-31+G*; 956.41 to 950.29 MHz, 6-311+G(2d,2p); 951.90 to 946.12 MHz, EPR-II/6-311+G(2d,2p)], and the effect on $A_{iso}(^{1}H)$ is ∼2 MHz [112.27 to 113.95 MHz, 6-31+G*; 107.86 to 109.64 MHz, 6-311+G(2d,2p); 120.50 to 122.46 MHz, EPR-II/6-311+G(2d,2p)]. Again, temperature effects are minimal, changing the computed hfs constants by only a few tenths of a megahertz for ^{31}P and ^{1}H. Clearly, there are still other factors to consider than just vibrational averaging. Thus, the aug-cc-pCVXZ and aug-cc-pV(X+d)Z families of basis sets were used to compute the hfs constants of H_2PO at the B3LYP/6-311+G(2d,2p) optimized geometry. Similar "convergence" trends to those that were observed for HPO_2^- were observed for H_2PO. While the aug-cc-pCVQZ value of $A_{iso}(^{31}P) = 963.33$ MHz is still significantly different from experiment (1023.43 MHz), the hfs constant of 111.51 MHz for ^{1}H is in close agreement with the experimental value of 109.27 MHz.

Solution effects on the Fermi contact terms for HPO_2^- and H_2PO were estimated using CPCM. These data are included in Tables 5 and 7. The shifts in the Fermi contact terms for HPO_2^- are toward experiment for both ^{31}P and ^{1}H with each basis set. With the 6-311+G(2d,2p) basis set, $A_{iso}(^{17}O) = -26.34$ MHz, $A_{iso}(^{31}P) = 1123.42$ MHz, and $A_{iso}(^{1}H) = 243.51$ MHz. The shifts in $A_{iso}(^{31}P)$ and $A_{iso}(^{1}H)$ for H_2PO are also toward experiment, with 6-311+G(2d,2p) values of −21.28 MHz (^{17}O), 1003.54 MHz (^{31}P), and 108.73 MHz (^{1}H).

The Fermi contact terms for the π radicals of *trans*- and *cis*-$HOPO^-$ are given in Tables 8 and 9, respectively. At the B3LYP/6-311+G*(2d,2p) level of theory, the hfs constants for *trans*-$HOPO^-$ are $A_{iso}(^{17}O_1) = -5.54$ MHz, $A_{iso}(^{17}O_2) = -18.30$ MHz, $A_{iso}(^{31}P) = 49.75$ MHz, and $A_{iso}(^{1}H) = -5.17$ MHz. For the cis-isomer, these values are −5.59 MHz ($^{17}O_1$), −17.88 MHz ($^{17}O_2$), 52.25 MHz (^{31}P), and −6.09 MHz (^{1}H). Vibrational averaging and temperature affect the computed hfs constants

TABLE 8: Isotropic Fermi Contact Couplings (MHz) for the $^2A''$ State of *trans*-$HOPO^-$ Using B3LYP[a]

trans-$HOPO^-$		$^{17}O_1$	$^{17}O_2$	^{31}P	^{1}H
6-31+G*		−8.81	−28.29	59.60	−5.27
	0 K	*−8.15*	*−28.62*	*62.81*	*−2.08*
	298 K	*−5.27*	*−30.89*	*61.33*	*−12.01*
	CPCM	−11.35	−27.00	74.03	−11.35
6-311+G(2d,2p)		−5.54	−18.30	49.75	−5.17
	0 K	*−4.99*	*−18.38*	*49.95*	*−2.60*
	298 K	*−3.08*	*−18.67*	*50.64*	*−6.34*
	CPCM	−7.44	−17.56	59.26	−5.67
EPR-II [H,O],		−7.40	−24.58	73.74	−6.13
6-311+G(2d,2p) [P]	0 K	*−7.00*	*−24.66*	*73.75*	*−4.90*
	298 K	*−6.54*	*−24.74*	*73.77*	*−3.49*
	CPCM	−9.51	−23.43	73.28	−6.60

[a] Vibrationally averaged values were computed at 0 and 298 K and are in italics. Solution phase values were estimated using CPCM.

TABLE 9: Isotropic Fermi Contact Couplings (MHz) for the $^2A''$ State of *cis*-$HOPO^-$ Using B3LYP[a]

cis-$HOPO^-$		$^{17}O_1$	$^{17}O_2$	^{31}P	^{1}H
6-31+G*		−9.11	−27.63	59.55	−5.93
	0 K	*−9.41*	*−27.68*	*59.46*	*−3.39*
	298 K	*−9.68*	*−27.73*	*59.40*	*−1.09*
	CPCM	−11.24	−26.42	73.12	−6.40
6-311+G(2d,2p)		−5.59	−17.88	52.25	−6.09
	0 K	*−6.09*	*−17.87*	*52.16*	*−2.78*
	298 K	*−6.62*	*−17.86*	*52.06*	*0.68*
	CPCM	−7.18	−17.16	60.69	−6.58
EPR-II [H,O],		−7.96	−24.06	71.00	−6.96
6-311+G(2d,2p) [P]	0 K	*−7.65*	*−24.51*	*69.15*	*−4.26*
	298 K	*−9.77*	*−26.84*	*59.32*	*63.54*
	CPCM	−8.74	−23.00	75.01	−7.33

[a] Vibrationally averaged values were computed at 0 and 298 K and are in italics. Solution phase values were estimated using CPCM.

TABLE 10: *g*-Factors for HPO_2^-, *trans*-$HOPO^-$, and *cis*-$HOPO^-$ Using B3LYP[a]

	HPO_2^-	HPO_2^-	*trans*-$HOPO^-$		*cis*-$HOPO^-$		
	($^2B_1$)	($^2A'$)	($^2A'$)	($^2A''$)	($^2A'$)	($^2A''$)	H_2PO
6-31+G*	2.002 52	2.002 44	2.002 33	2.001 17	2.002 27	2.001 90	2.002 70
	2.003 36	*2.003 42*		*2.001 95*		*2.001 85*	*2.002 67*
6-311+G(2d,2p)	2.002 55	2.002 41	2.002 33	2.000 97	2.002 27	2.000 89	2.002 70
	2.003 66	*2.003 21*		*2.001 84*		*2.001 75*	(2.002 66)
EPR-II [H,O],	2.002 46	2.002 40	2.002 33	2.000 37	2.002 27	2.000 03	2.002 69
6-311+G(2d,2p) [P]	*2.002 99*	*2.003 15*		*2.001 60*		*2.001 43*	(2.002 66)
		[2.003 03][b]					

[a] The experimental *g*-factor for HPO_2^- is in brackets. Values in solution are in italics. [b] Reference 16.

of $^{17}O_1$, $^{17}O_2$, ^{31}P, and ^1H by 2−4 MHz in the trans-isomer. In the cis-isomer, vibrational averaging and temperature have minimal effects on the Fermi contact terms of either O center. With the 6-31+G* and 6-311+G(2d,2p) basis sets, $A_{iso}(^{31}P)$ is not significantly affected by either of these two effects. However, with the EPR-II/6-311+G(2d,2p) basis set, vibrational averaging has an effect of ∼2 MHz at 0 K and ∼12 MHz at 298 K. The hfs constant of ^1H in *cis*-$HOPO^-$ is affected the most by vibrational averaging. At 0 K, there is a difference of ∼3 MHz, while, at 298 K, the difference is ∼5 MHz with the 6-31+G* and 6-311+G(2d,2p) basis sets and 56.58 MHz with the EPR-II/6-31+G(2d,2p) basis set.

D. *g*-Factors. The *g*-factors of the HPO_2^-, *trans*-$HOPO^-$, and *cis*-$HOPO^-$ radicals are given in Table 10. The *g*-factor is analogous to chemical shielding in NMR. The internal magnetic fields of bound unpaired electrons can shift or split the basic resonance line into multiple components. The orbital angular momentum of the unpaired electron contributes to the total magnetic moment, producing a shift in the *g*-factor from the free electron value of 2.002 32. In radical ions, *g*-factors are generally within 1−2% of the free electron value because the orbital angular momentum may be quenched. Using the EPR-II/6-311+G(2d,2p) basis set, this is observed for the radical anions studied here. The value of $\delta g_{obs} = 2.002\,40$ for $^2A'$ HPO_2^- is in good agreement with the experimental value of 2.003 03.[16] Using CPCM to estimate solution effects ($\delta g_{obs} =$ 2.003 15), the agreement with theory is even better. For *trans*- and *cis*-$HOPO^-$, the *g*-factors are 2.000 37 and 2.000 03, respectively, and with solution effects, these values are 2.001 60 (trans) and 2.001 43 (cis). Solution effects are much less pronounced for the computed *g*-factor for H_2PO. With the EPR-II/6-311+G(2d,2p) basis set, the *g*-factor is 2.002 69, and using the CPCM, this value is 2.002 66.

IV. Conclusions

The energetic ordering of the isomers of HPO_2 is *cis*-HOPO < *trans*-HOPO < HPO_2, while that of the anions is HPO_2^- < *cis*-$HOPO^-$ < *trans*-$HOPO^-$. The relative energies of the neutral systems are 0.0 kcal mol^{-1} (cis), 3.0 kcal mol^{-1} (trans), and 14.9 kcal mol^{-1} (HPO_2). The cis- and trans-anions lie ∼5 and ∼8 kcal mol^{-1}, respectively, higher than HPO_2^-. The minimum on the potential energy surface of the HPO_2^- radical is a pyramidal structure in C_s symmetry. Two radical anions are found for each cis- and trans-isomer of $HOPO^-$. The π radicals are lower in energy, while the σ radicals are really PO_2^- loosely associated with free H.

Vibrational averaging can be important for the theoretical prediction of Fermi contact terms for nonrigid radicals. This affects the computed hfs constants for H_2PO by 5−6 MHz for $A_{iso}(^{31}P)$ and 1−2 MHz for $A_{iso}(^1H)$, but $A_{iso}(^{17}O)$ is relatively unaffected. The Fermi contact terms for HPO_2^- show a smaller vibrational averaging effect for ^{31}P (∼2 MHz) but a larger effect for ^1H (8−20 MHz). $A_{iso}(^{17}O)$ remains relatively unaffected by vibrational averaging.

It is shown here that solvent effects are important to the accurate computation of hfs constants of the HPO_2^- and H_2PO radicals. With the 6-311+G(2d,2p) basis set, the computed Fermi contact terms for ^{31}P and ^1H in both radicals are in close agreement with experiment. In HPO_2^-, the values of $A_{iso}(^{31}P) = 1123.42$ MHz and $A_{iso}(^1H) = 243.51$ MHz compare to the experimental values of 1346 and 252 MHz, respectively. In HPO_2, the computed values of $A_{iso}(^{31}P) = 1003.54$ MHz and $A_{iso}(^1H) = 108.73$ MHz compare to the experimental values of 1023.43 and 109.27 MHz, respectively.

The Fermi contact terms computed for HPO_2^-, H_2PO, and P using B3LYP with the aug-cc-pCVXZ and aug-cc-pV(X+d)Z families of basis sets show that the convergence of $A_{iso}(^{31}P)$ is erratic and slow. While the more expensive CCSD(T) method produces hfs constants for the P atom that are in good agreement with the experimental value, the problems encountered using B3LYP show that using a basis set with a good description of the 1s core of P is critical for producing accurate theoretical values of $A_{iso}(^{31}P)$. Our attempts to make the core more flexible are successful in providing a more balanced basis set, as reflected by the convergence to experiment of the CCSD(T) results. However, the B3LYP values still do not show such convergence for this property of the P atom, which reflects the deficiency of the functional, which was after all parametrized from thermochemistry. Our modified aug-cc-pCVXZ basis sets do show good convergence for the Fermi contact term of the P center in HPO_2^-, although the converged value of $A_{iso}(^{31}P) =$ 1003.80 MHz is still different from experiment by ∼400 MHz.

Acknowledgment. N.R.B. is grateful to the Environmental Management Science Program of the Department of Energy (DOE) for partial support of this research and also thanks Ge Yan (Center for Computational Chemistry, The University of Georgia) for computing the spin densities of the P atom at the CCSD(T) level. This is Contribution No. NDRL-4516 from the Notre Dame Radiation Laboratory which is supported by Basic Energy Sciences at DOE.

References and Notes

(1) Werner, J. H.; Cool, T. A. *Chem. Phys. Lett.* **1997**, *275*, 278.
(2) Butcher, W. W.; Westheimer, F. H. *J. Am. Chem. Soc.* **1955**, *77*, 2420.
(3) Quin, L. D.; Hughes, A. N.; W. X.-P.; Dickinson, L. C. *J. Chem. Soc., Chem. Commun.* **1988**, 555.
(4) Bodalski, R.; Quin, L. D. *J. Org. Chem.* **1991**, *56*, 2666.
(5) Quin, L. D. *Coord. Chem. Rev.* **1994**, *137*, 525.
(6) Hinchliffe, A. *J. Mol. Struct.* **1981**, *71*, 349.
(7) Schoeller, W. W.; Lerch, C. *Inorg. Chem.* **1986**, *25*, 576.
(8) Lohr, L. L.; Boehm, R. C. *J. Phys. Chem.* **1987**, *91*, 3203.
(9) Mathieu, S.; Navech, J.; Barthelat, J. C. *Inorg. Chem.* **1989**, *28*, 3099.

(10) Withnall, R.; Andrews, L. *J. Phys. Chem.* **1988**, *92*, 4610.
(11) McCluskey, M.; Andrews, L. *J. Phys. Chem.* **1991**, *95*, 3545.
(12) Hildenbrand, D. L.; Lau, K. H. *J. Chem. Phys.* **1994**, *100*, 8373.
(13) Twarowski, A. *Combust. Flame* **1996**, *105*, 407.
(14) Mackie, J. C.; Bacskay, G. B.; Haworth, N. L. *J. Phys. Chem.* **2002**, *106*, 10825.
(15) Miller, T. M.; Stevens-Miller, A. E. *J. Phys. Chem.* **1991**, *95*, 1275.
(16) Morton, J. R. *Mol. Phys.* **1962**, *5*, 217.
(17) Behar, D.; Fessenden, R. W. *J. Phys. Chem.* **1972**, *76*, 1706.
(18) Werner, J. H.; Cool, T. A. *Combust. Flame* **1999**, *117*, 78.
(19) Korobeinichev, O. P.; Ilyin, S. B.; M. V. V., Shmakov, A. G. *Combust. Sci. Technol.* **1996**, *51*, 116.
(20) Bell, I. S.; Ahmad, I. K.; Hamilton, P. A.; Davies, P. B. *Chem. Phys. Lett.* **2000**, *320*, 311.
(21) Frisch, M. J.; Trucks, G. W.; Schlegel, H. B.; Scuseria, G. E.; Robb, M. A.; Cheeseman, J. R.; Zakrzewski, V. G.; Montgomery, J. A.; Stratmann, R. E.; Burant, J. C.; Dapprich, S.; Millam, J. M.; Daniels, A. D.; Kudin, K. N.; Strain, M. C.; Farkas, O.; Tomasi, J.; Barone, V.; Cossi, M.; Cammi, R.; Mennucci, B.; Pomelli, C.; Adamo, C.; Clifford, S.; Ochterski, J.; Petersson, G. A.; Ayala, P. A.; Cui, Q.; Morokuma, K.; Salvador, P.; Dannenberg, J. J.; Malick, D. K.; Rabuck, A. D.; Raghavachari, K.; Foresman, J. B.; Cioslowski, J.; Ortiz, J. V.; Baboul, A. G.; Stefanov, B. B.; Liu, G.; Liashenko, A.; Piskorz, P.; Komaromi, I.; Gomperts, R.; Martin, R. L.; Fox, D. J.; Keith, T.; Al-Laham, M. A.; Peng, C. Y.; Nanayakkara, A.; Challacombe, M.; Gill, P. M. W.; Johnson, B. G.; Chen, W.; Wong, M. W.; Andres, J. L.; Gonzalez, C.; Head-Gordon, M.; Replogle, E. S.; Pople, J. A. *Gaussian 98*; Gaussian, Inc.: Pittsburgh, PA, 2001.
(22) Frisch, M. J.; Trucks, G. W.; Schlegel, H. B.; Scuseria, G. E.; Robb, M. A.; Cheeseman, J. R.; Montgomery, J. A.; Vreven, T.; Kudin, K. N.; Burant, J. C.; Millam, J. M.; Iyengar, S. S.; Tomasi, J.; Barone, V.; Mennucci, B.; Cossi, M.; Scalmani, G.; Rega, N.; Petersson, G. A.; Nakatsuji, H.; Hada, M.; Ehara, M.; Toyota, K.; Fukuda, R.; Hasegawa, J.; Ishida, M.; Nakajima, T.; Honda, Y.; Kitao, O.; Nakai, H.; Klene, M.; Li, X.; Knox, J. E.; Hratchian, H. P.; Cross, J. B.; Adamo, C.; Jaramillo, J.; Gomperts, R.; Stratmann, R. E.; Yazyev, O.; Austin, A. J.; Cammi, R.; Pomelli, C.; Ochterski, J. W.; Ayala, P. Y.; Morokuma, K.; Voth, G. A.; Salvador, P.; Dannenberg, J. J.; Zakrzewski, V. G.; Dapprich, S.; Daniels, A. D.; Strain, M. C.; Farkas, O.; Malick, D. K.; Rabuck, A. D.; Raghavachari, K.; Foresman, J. B.; Ortiz, J. V.; Cui, Q.; Baboul, A. G.; Clifford, S.; Cioslowski, J.; Stefanov, B. B.; Liu, G.; Liashenko, A.; Piskorz, P.; Komaromi, I.; Martin, R. L.; Fox, D. J.; Keith, T.; Al-Laham, M. A.; Peng, C. Y.; Nanayakkara, A.; Challacombe, M.; Gill, P. M. W.; Johnson, B.; Chen, W.; Wong, M. W.; Gonzalez, C.; Pople, J. A. *Gaussian 03*; Gaussian, Inc.: Pittsburgh, PA, 2003.
(23) Becke, A. D. *J. Chem. Phys.* **1993**, *98*, 5648.
(24) Lee, C.; Yang, W.; Parr, R. G. *Phys. Rev. B* **1988**, *37*, 785.
(25) Rittby, M.; Bartlett, R. J. *J. Phys. Chem.* **1988**, *92*, 3033.
(26) Watts, J. D.; Gauss, J.; Bartlett, R. J. *Chem. Phys. Lett.* **1992**, *200*, 1.
(27) Watts, J. D.; Gauss, J.; Bartlett, R. J. *J. Chem. Phys.* **1993**, *98*, 8718.
(28) Barone, V.; Cossi, M. *J. Phys. Chem.* **1998**, *102*, 1995.
(29) Cossi, M.; Rega, N.; Scalmani, G.; Barone, V. *J. Comput. Chem.* **2003**, *24*, 669.
(30) Hehre, W. J.; Ditchfield, R.; Pople, J. A. *J. Chem. Phys.* **1972**, *56*, 2257.
(31) Francl, M. M.; Pietro, W. J.; Hehre, W. J.; Binkley, J. S.; Gordon, M. S.; Pople, J. A. *J. Chem. Phys.* **1982**, *77*, 3654.
(32) Frisch, M. J.; Pople, J. A.; Binkley, J. S. *J. Chem. Phys.* **1984**, *80*, 3265.
(33) Clark, T.; Chandrasekhar, J.; Schleyer, P. v. R. *J. Comput. Chem.* **1983**, *4*, 294.
(34) Hehre, W. J.; Radom, L.; Schleyer, P. v. R.; Pople, J. A. *Ab Initio Molecular Orbital Theory*; Wiley: New York, 1986.
(35) McLean, A. D.; Chandler, G. S. *J. Chem. Phys.* **1980**, *72*, 5639.
(36) Barone, V. In *Recent Advances in Density Functional Methods, Part I*; Chong, D. P., Ed.; World Scientific Publishing Co.: Singapore, 1996.
(37) Woon, D. E.; Dunning, T. H. *J. Chem. Phys.* **1995**, *103*, 4572.
(38) Kendall, R. A.; Dunning, T. H.; Harrison, R. J. *J. Chem. Phys.* **1992**, *96*, 6796.
(39) Dunning, T. H.; Peterson, K. A.; Wilson, A. K. *J. Chem. Phys.* **2001**, *114*, 9244.
(40) van Doren, J. M.; Viggiano, A. A.; Morris, R. A.; Stevens-Miller, A. E.; Miller, T. M.; Paulson, J. F.; Deakyne, C. A.; Michels, H. H.; Montgomery, J. A., Jr. *J. Chem. Phys.* **1993**, *98* (10), 7940.
(41) Wesolowski, S. S.; Brinkmann, N. R.; Valeev, E. F.; Schaefer, H. F.; Repasky, M. P.; Jorgensen, W. L. *J. Chem. Phys.* **2002**, *116*, 112.
(42) Dunning, T. H. *J. Chem. Phys.* **1989**, *90*, 1007.
(43) Woon, D. E.; Dunning, T. H. *J. Chem. Phys.* **1993**, *98*, 1358.
(44) Wilson, A. K.; van Mourik, T.; Dunning, T. H. *THEOCHEM* **1996**, *288*, 339.
(45) van Mourik, T.; Dunning, T. H. *Int. J. Quantum Chem.* **2000**, *76*, 205.
(46) Tackett, B. S.; Clouthier, D. J. *J. Chem. Phys.* **2002**, *117*, 10604.
(47) Knight, L. B.; Jones, G. C.; King, G. M.; Babb, R. M.; McKinley, A. J. *J. Chem. Phys.* **1995**, *103*, 497.
(48) Carmichael, I. *J. Phys. Chem. A* **1997**, *101* (25), 4633.
(49) Nguyen, M. T.; Creve, S.; Eriksson, L. A.; Vanquickenborne, L. G. *Mol. Phys.* **1997**, *91*, 537.
(50) Godbout, N.; Salahub, D. R.; Andzelm, J.; Wimmer, E. *Can. J. Chem.* **1992**, *70*, 560.
(51) Barone, V.; Adamo, C.; Brunel, Y.; Subra, R. *J. Chem. Phys.* **1996**, *105*, 3168.
(52) Barone, V.; Grand, A.; Minichino, C.; Subra, R. *J. Chem. Phys.* **1993**, *99*, 6787.
(53) Barone, V.; Grand, A.; Minichino, C.; Subra, R. *J. Phys. Chem.* **1993**, *97*, 6355.
(54) Barone, V.; Minichino, C.; Faucher, H.; Subra, R.; Grand, A. *Chem. Phys. Lett.* **1993**, *205*, 324.
(55) Hug, G. L.; Camaioni, D. M.; Carmichael, I., submitted for publication.
(56) Nguyen, M. T.; Ha, T.-K. *Chem. Phys.* **1989**, *131*, 245.
(57) de Waal, B. F. M.; Aagaard, O. M.; Janssen, R. A. J. *J. Am. Chem. Soc.* **1991**, *113*, 9471.
(58) Cramer, C. J.; Lim, M. H. *J. Phys. Chem.* **1994**, *98*, 5024.
(59) Nguyen, M.; Creve, S.; Vanquickenborne, L. *J. Phys. Chem.* **1997**, *101*, 3174.
(60) Wesolowski, S. S.; Johnson, M. E.; Leininger, M. L.; Crawford, T. D. *J. Chem. Phys.* **1998**, *109*, 2694.
(61) Hirao, T.; Saito, S.; Ozeki, H. *J. Chem. Phys.* **1996**, *105*, 3450.
(62) Hunter, S. J.; Hipps, K. W.; Francis, A. H. *Chem. Phys.* **1979**, *39*, 209.